International Journal of Rock Mechanics & Mining Sciences 67 (2014) 164–169

Contents lists available at ScienceDirect

International Journal of Rock Mechanics & Mining Sciences

journal homepage: www.elsevier.com/locate/ijrmms

Experimental study of gravity flow under confined conditions

Raúl L. Castro [a,*], Miguel A. Fuenzalida [a], Fernando Lund [b]

[a] Block Caving Laboratory, Advanced Mining Technology Center, University of Chile, Santiago, Chile
[b] Physics Department, Faculty of Physical Sciences and Mathematics, University of Chile, Santiago, Chile

ARTICLE INFO

Article history:
Received 26 March 2013
Received in revised form
10 January 2014
Accepted 20 January 2014
Available online 7 March 2014

Keywords:
Gravity flow mechanics
Isolated draw
Interlocking arching
Hang-ups
Secondary fragmentation

ABSTRACT

Caving methods rely on gravity to break up and transport large amounts of ore and waste. Massive underground mining is becoming even more prevalent due to the depletion of surface mining reserves. It is thus relevant to study the gravity flow mechanisms that will occur at deeper levels. Despite the importance of gravity flow, there is a lack of quantification of the influence that confinement (the weight of the ore column) has on the secondary fragmentation and the caved rock ability to flow. This paper presents the design and results of an experimental setup used to investigate the flow mechanisms of cohesionless material when drawing from a single drawpoint under confinement. Experimental results showed that the flowability of the material is influenced by the rock fragment size, dimension or diameter of the opening and the vertical load applied. Secondary fragmentation is mainly influenced by the vertical load applied and the size distribution of the fragmented rock. Finally, flowability mechanisms are presented in terms of a state graph and a hang-up frequency graph, both of which could be used for the design of openings in mining.

1. Introduction

Block caving is an underground bulk mining method that offers continued production at a comparably high rate, with low operating costs. Block caving relies on gravity to break up and transport large amounts of ore. In order to achieve a continued high rate of production, there are certain key aspects that need to be taken into account in the design of a caving operation. One of these is the fragmentation that can result from the induced stresses during caving propagation and the associated movement of the caved rock to the drawpoints. Another, related aspect, is the flow capability of the caved rock [1,2].

Flowability can be defined as the flow condition or ability of a granular material to flow under a given set of material properties, infrastructure geometry and stress conditions. In the past, flowability has been classified into free flow, intermittent flow, and no-flow. The methods for estimating flowability have been derived from observations at mine sites, and experiments have shown particle size, opening size and fines content to be key parameters. The flowability, in turn, defines the size of a key mine infrastructure, the diameter of ore passes or drawpoints [3–6]. In the case of intermittent flow it is useful for mine operations to have a quantification of interferences or hang ups, that determine the intermittency, in terms of a number of hang-ups per 1000 t drawn and in terms of average extracted tonnage in between hang-ups [7].

The process of fragmentation in a cave mine involves both primary and secondary fragmentations. Primary fragmentation is attributable to the induced stresses during caving propagation while secondary fragmentation results from the breakage process that occurs as the blocks move down through the draw column to the drawpoints [1].

In terms of the mechanisms of secondary breakage, Pierce [8] has postulated that there are three main modes of breakage in a cave: impact breakage within the air gap at the top of the cave; compression breakage within stagnant zones of the cave resulting in block splitting (a fragment breaks into two or more pieces); and shear-driven breakage within movement zones resulting in corner rounding. The relative influence of each kind of breakage remains uncertain.

To date, knowledge on the mechanisms of gravity flow in caving mines (flowability and secondary fragmentation) has been gained through mine data analysis, numerical modeling and physical modeling. Physical models have the advantage to be controlled experiments that can be used to understand the mechanisms of flow. Significant efforts have been made to build physical models to understand the mechanisms of gravity flow in caving mines including large-scale 3D models [9,10]. However, even the large physical models studied to date do not achieve full similitude to a real operation and cannot be used to understand breakage and compaction since the vertical loads that have been used are relatively small (about 32 kPa) when compared to the strength of the granular media (100–150 MPa).

* Corresponding author. Tel.: +56 2 2978 4497.
E-mail address: rcastro@ing.uchile.cl (R.L. Castro).

http://dx.doi.org/10.1016/j.ijrmms.2014.01.013
1365-1609

Under those conditions, hang-ups as a result of mechanical arches, breakage and compaction are not observed. This article addresses this shortcoming of previous experiments: by the use of confined flow experiments – whose set up and initial results are presented below – we aim at the understanding of these important mechanisms.

2. Laboratory equipment for confined granular flow

2.1. Equipment design

One of the main objectives of this research was to design a set of experiments where flow tests could be performed under large vertical stresses [11]. The confined flow set up consists of a steel cylinder, an extraction system and a hydraulic press (Fig. 1). The steel cylinder has 340 mm inner diameter, and can stand an applied pressure of 14 MPa. The application of the load is through a 1800 KN hydraulic press. The cylindrical geometry of the steel cylinder was chosen to avoid boundary effects related to arching, and stress concentrations at corners. In terms of arching the diameter was chosen so that it could handle up to 12 mm particles. Consequently the width to particle size ratio is 28, which is well above the soil mechanics standards for triaxial tests of 10 particle sizes [12]. In terms of the flow characteristics, the diameter of the flow zone was always smaller than 340 mm so it was an isolated draw. The height of the cylinder was 700 mm in order to hold the desired volume of gravel and to comply with the 2:1 height to width ratio. The base of the cylinder had a drawpoint located in the center of the model so that the flow zones would not intersect the model's walls. The diameter of the drawpoint (d_w) was set at 100 mm. A steel extraction system was built to extract the material (Fig. 1b), containing a wedge that pushes the material out of the cylinder.

2.2. Preparation of specimens and procedure

The experiment required the application of an axial load, ranging from 0 to 1800 KN, which is the maximum load capacity of the hydraulic press. The piston is brought to rest against the surface of the sample. The press is started and when it reaches the required load, the extraction process begins and the load is kept constant. One of the questions to be answered before the tests were run was the magnitude of the vertical load that ought to be applied to our press in order to mimic the vertical stresses that occur when a large fragmented pile of rock develops after the cave. In order to quantify the vertical stress in a granular material we use Janssen's formula [13]

$$\sigma_v = \frac{R_h \gamma}{k \tan \phi}[1 - e^{k(\tan \phi) z/R_h}], \quad (1)$$

where σ_v is the vertical stress, R_h is hydraulic radius (area/perimeter) of the area of draw under analysis, γ and ϕ are the density and friction angle of the fragmented rock, z is the height of the caved rock pile, and k is an earth pressure related constant whose value depend on the mode of failure of the granular material. Taking $R_h = 70$ m; $\gamma = 2200$ kg/m^3 and $\phi = 38^\circ$, $k = 1 - \sin\phi = 0.38$, we tabulate the resulting stress together with the equivalent press load for the geometry of our apparatus in Table 1. We conclude that our experiment represents the conditions of a cave pile of more than 1000 m height, which is considered deep.

The procedure consisted of applying a constant axial load during the test until a determined quantity of material was extracted from the drawpoint. Once the model media was tested, the cylinder was removed from the press and placed in a horizontal position. Then it was opened and "cut in half" in order to observe flow zones and to take samples for fragmentation

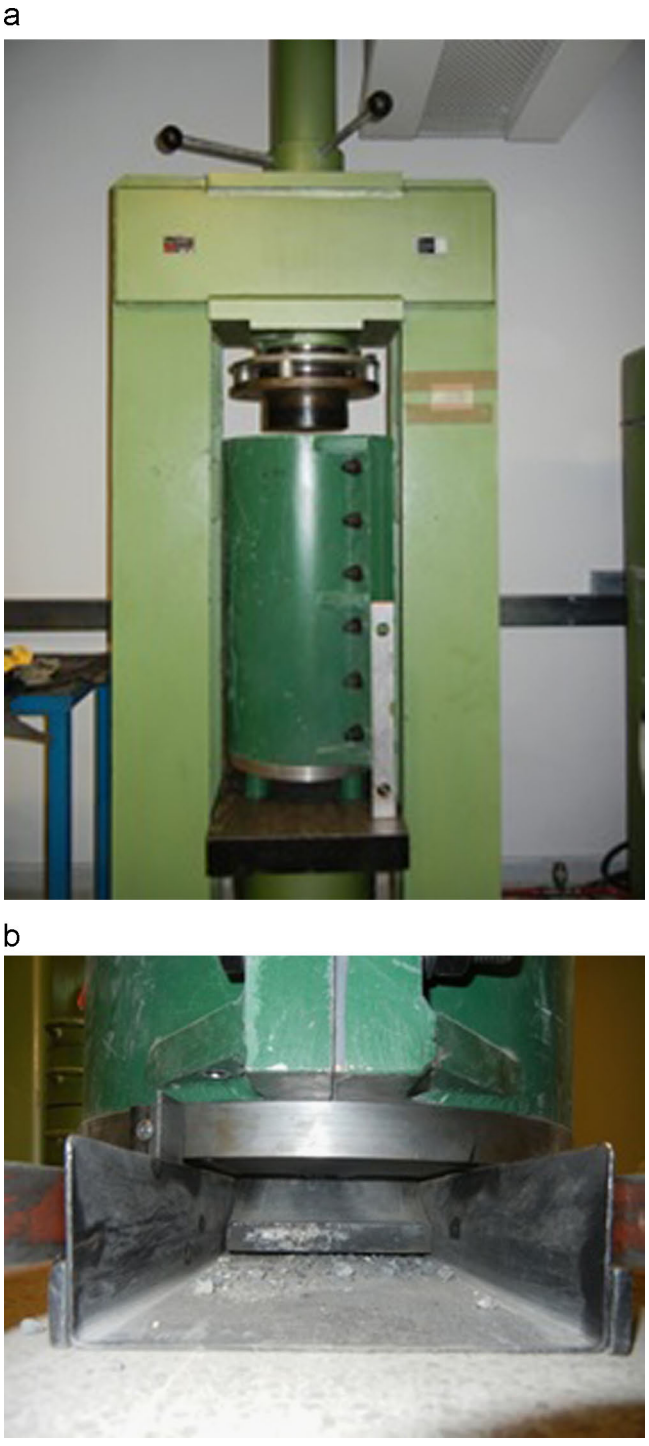

Fig. 1. Hydraulic press and steel cylinder (a) and the cylinder (b).

Table 1
Range of loads according to vertical stresses using Eq. (1).

Depth	Mean vertical stress (MPa)	Press load (KN)
100	1.76	159
200	2.91	264
300	3.66	332
500	4.47	406
700	4.82	437
1000	5.00	454
1500	5.07	460

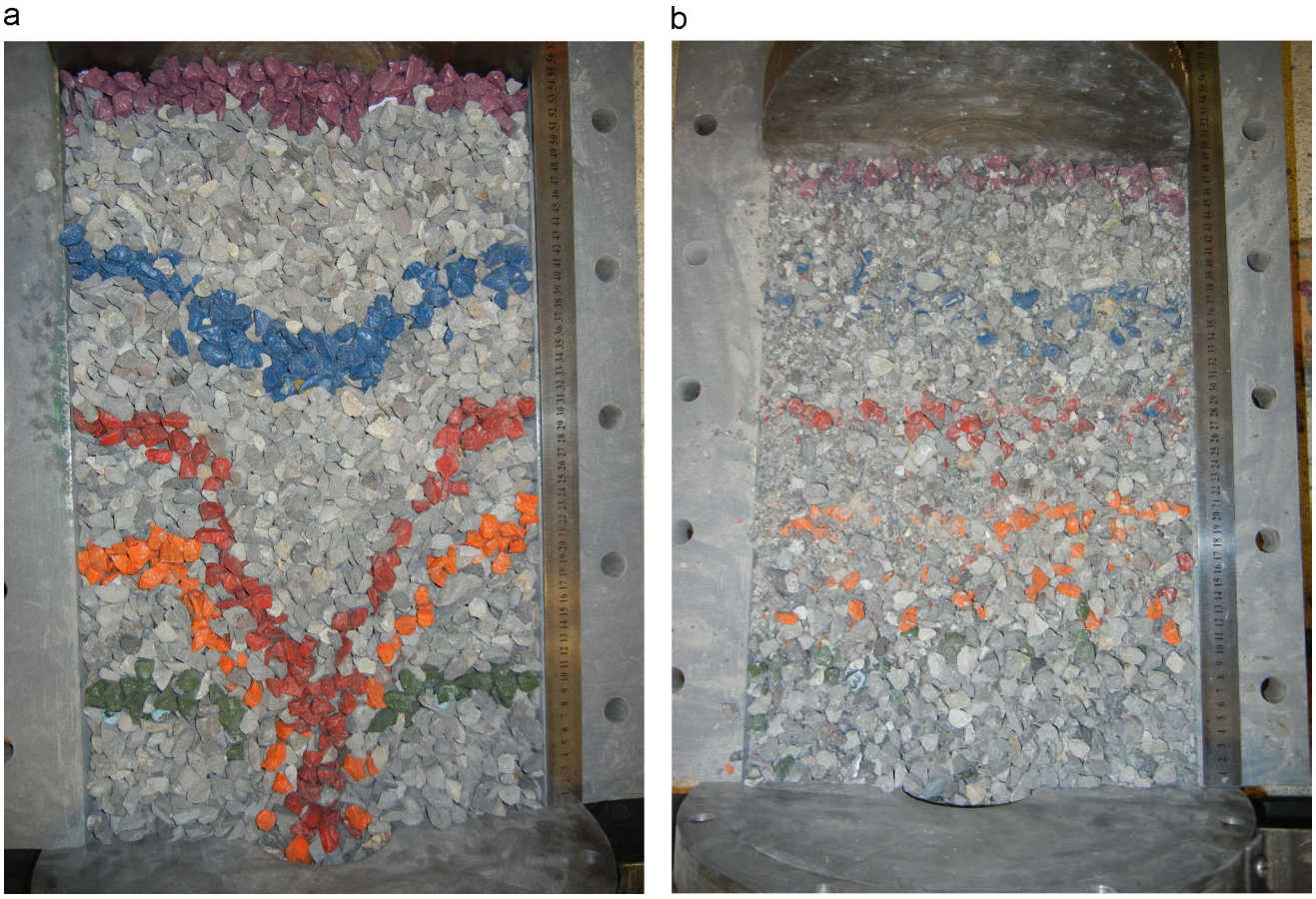

Fig. 2. (a) Flow zone observed at the end of experiment, d_{50}=12 mm. (b) Flow zone observed at the end of experiment, 13.2 MPa.

analysis. Due to the 3D configuration of the physical model, the material was surrounded on all sides and could not be visually inspected from the outside. Therefore, in order to determine the extraction zone, painted numbered tracers were positioned inside the model and recovered at the drawpoint (Fig. 2). In order to determine the movement zone (flow zone), painted markers with different colors were placed every 10 cm (Fig. 2).

Regarding the flowability measurements for these tests, four modes of flow were recorded. (a) **Free Flow:** the material flows freely through the point of extraction without interruption. (b) **Intermittent Flow:** the material flows with intermittent interruptions due to arches formed by mechanical material compaction. They break apart due to the vertical force applied by the hydraulic press. (c) **Assisted Flow:** in order for the material to flow, manual intervention is needed to disrupt the mechanical arches. (d) **No Flow:** the material is completely stagnant, even when disturbed manually.

2.3. Model media

The tests described in this paper were conducted using crushed gravel. During the experimental phase, three model media were tested, two with a fairly narrow distribution of different particle sizes (d_{50}=6 mm and 12 mm) and a third with a wide distribution (d_{50}=8 mm), as indicated in Table 2. The ratios between particle size and the opening diameter were 6, 8 and 12 respectively. The cumulative size distribution curves for the different particle sizes are presented in Fig. 3.

Other properties of the media under study were measured and are summarized in Table 2. In this the uniformity index is the ratio between the sixty and ten percent particle passing size, and the porosity is the amount of voids in the granular media before the tests.

Table 2
Summary of the Characteristics of the Model Media used in the Experiments.

Media	Mean size, d_{50}	Uniformity index, Cu	Swell, n [%]	Drawpoint/particle size ratio, w/d_{50}
6 mm	6.25	1.5	44	16
8 mm	8.17	4.1	40	12
12 mm	12.59	1.17	44	8

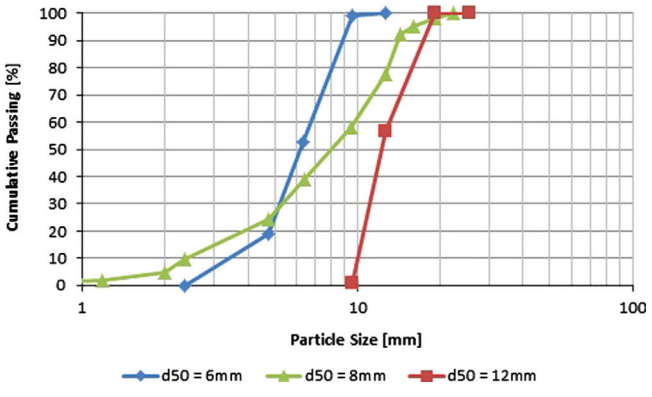

Fig. 3. Particle size distribution for the model media.

The shear strength characteristics of the tested materials were determined using a large (300 mm × 300 mm) shear box. Samples

were subjected to different normal forces ranging from 50 to 980 KPa. It was observed that cohesion was zero and the friction angle reached a value of 42°. It was also found that for normal stresses above 480 KPa the gravel showed a low angle of dilatancy, indicating that above this value the material would break due to compaction. Other mechanical properties for the model media are shown in Table 3.

3. Experimental results

A total of twenty-three experiments were performed to quantify confined flow, with results that are presented in Table 4. Each one of the three batches of gravel (6, 8, and 12 mm) was loaded to 2, 3, 5.8 and 12 MPa, twice, with the exception of the 8 mm batch that was loaded to 5.8 MPa only once. After each loading material was extracted from the drawpoint, as explained in Section 2, and its size distribution was determined (Table 4, columns 3, 4 and 5). Also, the flow condition was noted in each case (Table 4, column 6). As expected, there is a general trend that larger particles flow with mode difficulty. Importantly, the data shows that as the vertical load increases the mean size of the extracted material decreases, and its dispersion increases. An increased load also results in a more difficult flow condition. Reduction was quantified for the mean size in terms of the initial ($d_{50,i}$) and final size ($d_{50,f}$) as

$$R_{50} = \frac{d_{50,f} - d_{50,i}}{d_{50,i}} \quad (2)$$

The size distributions of particles before and after the tests are presented in Figs. 4–6. As expected, the greater the vertical load applied, the greater the degree of particle breakage. Regarding the influence of the size distribution on the breakage, the results show that breakage occurs mainly for smaller particles generating a considerable amount of fines. However in the wide distribution, breakage occurs among all particle sizes reducing the overall mean size.

Table 3
Summary of the characteristics of the model media used in the experiments.

		Gravel
Point strength Index I_{s50} (ASTM D5731-08)	**[MPa]**	6.3 (± 1.6)
Particle shape	**Sphericity** **Roundness** **Regularity**	0,65 0,51 0.58
Solid density	**[ton/m^3]**	2.69
Residual friction angle	**[deg.]**	42
Peak friction angle	**[deg.]**	48
Wall friction angle	**[deg.]**	20

4. Flowability assessment of caved rock

From the experiments and data collected from the literature a flowability graph was designed as shown in Fig. 7. In this the different flow states of the caved rock is a function of vertical

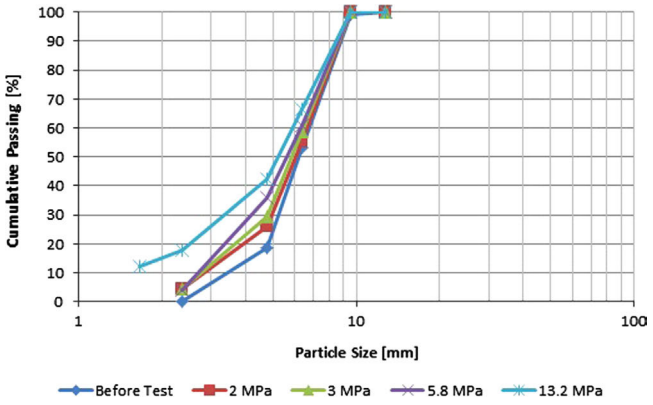

Fig. 4. Size distribution for 6 mm media.

Table 4
Summary of experimental results.

Exp.	σ_v [MPa]	d_{50i} [mm]	d_{50f} [mm]	R_{50}[%]	Flow condition	Interferences [g/hang-up]	Standard dev. [g/hang-up]
1.1.A	2	6.25	6.1	2.4	Free	955	156
1.2.A	3	6.25	5.93	5.1	Intermittent	625	0
1.3.A	5.8	6.25	5.7	8.8	Intermittent	703	559
1.4.A	12	6.25	5.29	15.3	Assisted	489	105
1.1.B	2	6.25	5.95	4.8	Free	INF	–
1.2.B	3	6.25	6.07	2.9	Free	INF	–
1.3.B	5,8	6.25	5.95	4.8	Intermittent	680	160
1.4.B	12	6.25	5.29	13.5	Assisted	546	127
2.1.A	2	8.17	7.07	13.5	Intermittent	ND	ND
2.2.A	3	8.17	7.06	13.6	Intermittent	ND	ND
2.3.A	5.8	8.17	6.77	17.1	Assisted	ND	ND
2.4.A	12	8.17	6.4	21.7	Assisted	ND	ND
2.1.B	2	8.17	7.82	4.3	Intermittent	ND	ND
2.2.B	3	8.17	7.71	5.6	Intermittent	ND	ND
2.4.B	12	8.17	6.51	20.3	Assisted	ND	ND
3.1.A	2	12.59	12.48	0.9	Intermittent	778	133
3.2.A	3	12.59	12.31	2.2	Assisted	383	225
3.3.A	5,8	12.59	12.31	2.2	Assisted	403	229
3.4.A	12	12.59	11.83	6.1	No flow	0	0
3.1.B	2	12.59	12.4	1.5	Free	INF	–
3.2.B	3	12.59	12.23	2.9	Assisted	493	445
3.3.B	5.8	12.59	11.85	5.8	Assisted	303	99
3.4.B	12	12.59	11.15	11.4	No flow	0	–

ND: no data was measured; INF hang ups were not observed.

stress and d_w/d_{50} ratios. This was built using the above experiments and also the results published by Hustrulid [3] on ore pass designs, which were conducted under near zero vertical loads. The points for nonzero vertical load are extracted from Table 4.

Fig. 7 could have applications to cave mining. For example let us consider that due to design, the ratio between drawpoint to particle size (d_w/d_{50}) is equal to 5. In this case we would expect to have intermittent-flow with cero vertical load. As the vertical load increases (see Eq. (1) for reasons for this) the flow would change to assisted flow at about 2 MPa while at 6 MPa would be in a no flow condition. In this case the flow condition could be changed from no-flow to intermittent-flow by increasing the drawpoint so that $d_w/d_{50} > 6$.

In those of our experiments that presented intermittent flow, hangups occurred depending on the vertical load. The influence of stresses on the hang up frequency was quantified measuring the mean amount of fragmented rock drawn before an arch occurs. As noted in Fig. 8, the amount of mass drawn before a hang up

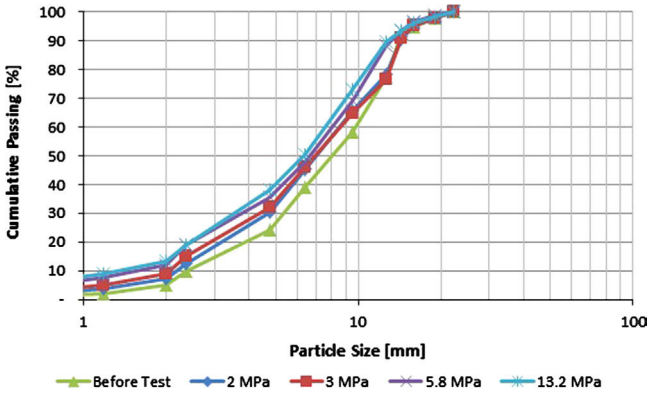

Fig. 5. Size distribution for 8 mm media.

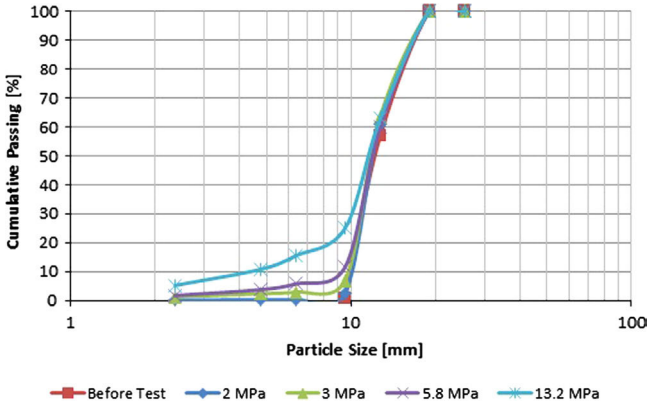

Fig. 6. Size distribution for 12 mm media.

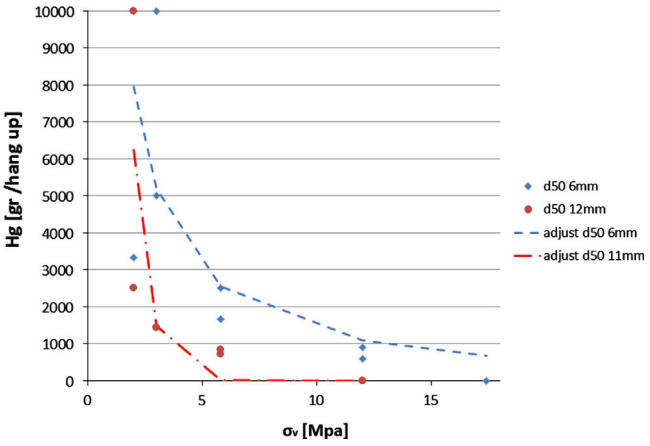

Fig. 8. Hang-up frequency as a function of vertical load.

Table 5
Fitted parameters for hang up frequency.

Media	d_w/d_{50}	H_{go} (gr/hang up)	r (adim)
6 mm	12.6	16.498	0.02
12 mm	6.25	111.125	1.44

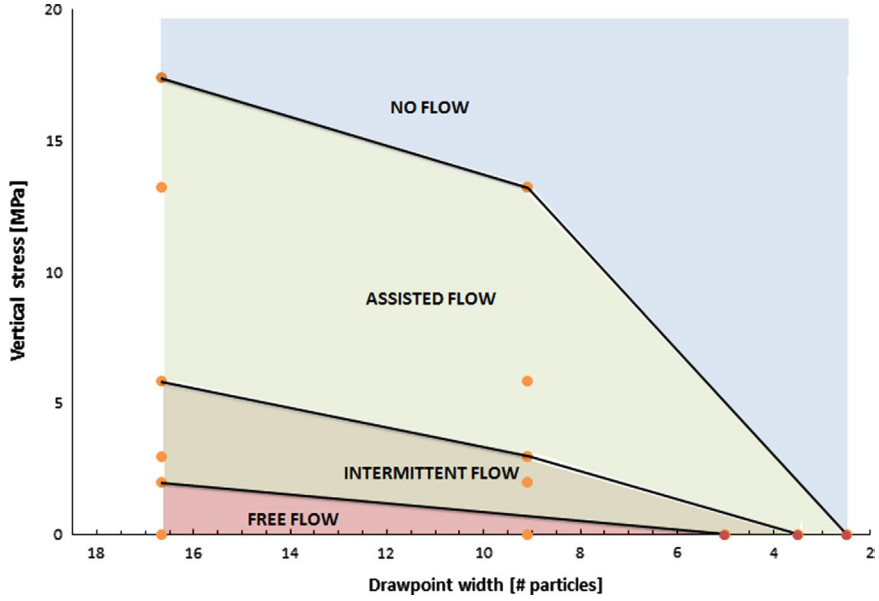

Fig. 7. Flow-ability graph of caved rock.

occurs decreases as the vertical stress increases in a non-linear fashion. Also, as was expected, as the d_w/d_{50} ratio increases there is a reduction in the hang-up frequency. Fig. 8 shows a fitted exponential equation represented as follows:

$$H_g = H_{go}\exp(-r\sigma_v) \quad (3)$$

where H_g is the amount of material that was drawn before a hang up occurs, H_{go} and r are fitted parameters which are related to the hang up frequency of the fragmented rock under zero vertical stress and the rate at which the flowability reduces with the load respectively. Thus a larger value of r would mean larger decrease on the flowability with the increase on vertical stress. Table 5 shows the value of the fitted parameters for the media analyzed in these experiments.

5. Conclusions and discussion

The applied vertical stress was found to have a considerable effect on the flowability and fragmentation of the media using a set up that simulates the vertical loads that could occur in caving mines. Changes include reduction in size and flowability of fragmented rock for increased loading. The flowability has been measured using experiments and a state graph has been derived. From this graph, the flowability of a given fragmented material could be classified for a given vertical stress and particle/opening size ratio.

Flowability was quantified for the case of intermittent flow in terms of hang up frequency. The hang up frequency depends on the particle to opening size ratio, and on the vertical stress.

The experimental results indicate that large vertical stresses induce secondary fragmentation due to compaction during the gravity flow of the caved rock. The greater the vertical stress applied, the greater the degree of breakage. The mean size could reduce up to 20% depending on the vertical load applied.

The experimental set up was successful in understanding the basic mechanisms of flow under confinement. There is more research to be conducted in the future to further understand the practical implications of flow under vertical load for mine design purposes. Topics to be investigated include the influence of fines and of water, as well as the influence of the geometry of drawbells and equipment type on hang up frequency for comparison with mine scale information. There is also research to be done in terms of the modeling of breakage and hang ups. Eq. (3) would need further refinement to be used as design criteria for caving. In the meantime this type of tests could be considered to be part of a standard for mine design applications when quantifying confined flow. To this end, the influence of scale and diameter of the cylinder should be considered. Large physical models could still be used to understand the kinematic of flow including fines migration and production rates. These topics are currently under research and will be submitted for publication in the near future.

Acknowledgments

This paper describes a component of the work carried out under the Project “Engineering Fundamentals of Block Caving” run by the University of Chile's Advanced Mining Technology Center (AMTC) and funded by the Chilean Government through Conicyt. The authors would also like to acknowledge Mr. Rene Gomez for helping in carry out many of the tests published in this article.

References

[1] Brown ET. Block caving geomechanics. 2nd ed. Brisbane: Julius Kruttschnitt Minerals Research Center, University of Queensland; 2007.
[2] Chitombo GP. Cave mining – 16 years after Laubscher's 1994 paper “Cave mining – State of the Art”. In: Potvin Y, editor. Caving 2010. Australia: Perth; 2010. p. 45–61.
[3] Hustrulid W, Sun C. Some remarks on ore pass design guidelines. In: Karzulovic A, Alfaro M, editors, Proceedings of MassMin, Santiago, Chile; 2004. p. 301–8.
[4] Kvapil R. Gravity flow of granular materials in hoppers and bins. Int J Rock Mech Sci 1965;35:41–2.
[5] Hadjigeorgiou J, Lessard JF. Numerical investigations of ore pass hang-up phenomena. Int J Rock Mech Min Sci 2007;820:834–44.
[6] Beaus M, Pariseau W, Stewart B, Iverson S. Design of ore pass. In: Hustrulid W, Bullock R, editors. Underground mining methods. Litteton, Colorado, USA: SME; 2001. p. 627–34.
[7] Maass S. Technology alternatives to solve hang ups on drawbells [Masters thesis]. Santiago: University of Chile; 2013 (in Spanish).
[8] Pierce M. A hybrid methodology for secondary fragmentation prediction in cave mines. In: Potvin Y, editor. Caving 2010. Australia: Perth; 2010. p. 567–81.
[9] Castro R, Trueman R, Halim A. Study of isolated draw zones in block caving mines by means of a large 3D physical model. Int J Rock Mech Min Sci 2007;44:860–70.
[10] Trueman R, Castro R, Halim A. Study of multiple draw-zone interaction in block caving mines by means of a large 3D physical model. Int J Rock Mech Min Sci 2008;45:1044–51.
[11] Fuenzalida M. Study of the confined gravity flow and its application to caving. [Master's thesis]. Santiago, Chile: University of Chile; 2012 ([in Spanish]).
[12] ASTM D7181. Method for consolidated drained triaxial compression test for soils. International; 2011.
[13] Janssen H. Experiments regarding grain pressure in silos. In: Karzulovic A, Alfaro M, editors, Proceedings of MassMin. Santiago, Chile; 2004. p. 293–300.